Electronic structure of solid uranium tetrafluoride UF$_4$

A. Yu. Teterin,* Yu. A. Teterin, K. I. Maslakov, and A. D. Panov

RRC Kurchatov Institute, Moscow, 123182, Russia

M. V. Ryzhkov†

Ural Department of RAS, Institute of Solid State Chemistry, Ekaterinburg, Russia

L. Vukcevic‡

Faculty of Natural Sciences and Mathematics, University of Montenegro, Podgorica, Serbia and Montenegro

X-ray photoelectron spectra (XPS) and conversion electron spectra of the outer (0–15 eV) and inner (15–40 eV) valence electrons for UF$_4$ were measured. Relativistic X_α discrete variation (RX_α DV) calculation data for the UF$_8^{4-}$ (C$_{4v}$) cluster reflecting uranium close environment in solid UF$_4$ were used for the quantitative interpretation of the fine spectral structure. Quantitative agreement between the experimental and theoretical data was established. The U 5f electrons ($\approx$1 U 5f electron) were shown to participate directly in the chemical bond formation. This U 5f electron was shown to be delocalized within the outer valence molecular orbitals (OVMO) range (1–15 eV). The other U 5f electrons were shown to be localized and to participate weakly in the chemical bond formation. The XPS line associated with these electrons was observed at 3.8 eV. The vacant U 5f states are generally delocalized in the range of the low positive energies (0–7 eV). The contribution of the U 6p electronic density to the molecular orbitals of UF$_4$ was experimentally and theoretically evaluated. The U 6p electrons were experimentally shown to participate significantly (0.6 U 6p electrons) in the formation of the OVMO beside the formation of the inner valence molecular orbitals (IVMO). IVMO composition and sequence order in the binding energy range 15–40 eV in UF$_4$ were determined.

I. INTRODUCTION

X-ray photoelectron spectroscopy (XPS) studies of uranium, uranium fluorides and other compounds have revealed a complex fine structure in the low binding energy (E_b) range.[1–6] For example, the XPS from solid uranium tetrafluoride UF$_4$ and uranyl fluoride UO$_2$F$_2$ show a great difference in the structures of all the valence binding energy (E_b) range 0–40 eV (Refs. 5 and 7) since uranium U^{6+} ion's electronic configuration in UO$_2$F$_2$ is {Rn}5f^0, and that of U^{4+} one in UF$_4$ is {Rn}5f^2, where {Rn}—radon electronic configuration. Therefore, the XPS from UF$_4$ exhibits a relatively sharp (1.5 eV wide) peak at E_b=3.8 eV attributed to the U 5f electrons weakly participating in the chemical bond. The XPS from UO$_2$F$_2$ does not exhibit this peak.

The XPS peaks in the E_b range 0–40 eV from uranium fluorides and other compounds were observed[7,8] to be several eV wide. For example, for UF$_4$, the F 1s peak's (E_b=685.3 eV) full width at half-maximum (FWHM) is Γ=1.3 eV, while the corresponding F 2s peak (E_b=29.9 eV) is 3.7 eV wide and structured. The extra structure was observed on the both sides from the expected single F 2s peak. This F 2s widening (relative to the F 1s FWHM) contradicts the uncertainty ratio $\Delta E \Delta \tau \sim h/2\pi$, where ΔE—natural width of the level from which an electron was removed, $\Delta \tau$—lifetime of a hole and h—Plank's constant. Since the hole lifetime ($\Delta \tau$) decreases as the absolute energy of a level grows, the XPS atomic peaks are expected to narrow as the electron binding energy decreases. In case of UF$_4$ and UO$_2$F$_2$ the picture is reversed. One of the reasons for the XPS peak widening in the binding energy range 0–40 eV was found to

be the formation of molecular orbitals (MOs).[8–10] These MOs form generally from the An 6p and L ns atomic shells of actinides and ligands (L). The formed MOs can be subdivided into the outer valence molecular orbitals (OVMO) (0–15 eV E_b) and inner valence molecular orbitals (IVMO) (15–40 eV E_b). Practically, the XPS spectra reflect the structure of the valence band (0–40 eV) and are observed as several eV wide bands. It was shown that under favorable conditions the IVMO could form in compounds of any elements of the periodic table.[8–11]

According to the earlier suggestions, the An 5f electrons are supposed to get promoted, for example, to the An 6d atomic orbitals before the chemical bond formation. However, the theoretical calculations show that the An 5f atomic shells can participate directly in the MO formation in actinide compounds.[7,8] Therefore, it is important to determine the experimental An 5f and An 6p partial electronic densities.

The qualitative identification of the XPS data for uranium tetrafluoride[7] allowed a qualitative interpretation of the conversion electron (CES) (Ref. 12) and x-ray O$_{4,5}$(U) emission (XES) (Ref. 13) spectral structures. The absence of the relativistic electronic structure calculations did not allow a correct interpretation of these spectral structures. The calculations are too complicated because of the fact that uranium environment in solid tetrafluoride cluster (UF$_8^{4-}$ of symmetry group D_{4d}) is too complex. The authors of Ref. 14 made an attempt to interpret qualitatively the electronic structure of solid UF$_4$ on the basis of the relativistic calculation results for the UF$_4$ (T_d) cluster reflecting uranium environment in the gaseous tetrahedral molecule. Earlier the XPS, CES and

$O_{4,5}(U)$ XES results taking into account the relativistic calculations were used for the quantitative evaluation of the partial densities of the U $6p$ and $5f$ electronic states in the binding energy range 0–40 eV in UO_2,[15] γ-UO_3,[16] and UO_2F_2.[17]

This work analyzes the fine low binding energy (0–40 eV) high resolution XPS and CES structures from UF_4 taking into account relativistic X_α discrete variation method (RX_α DVM) electronic structure calculation for the UF_8^{4-} (C_{4v}) cluster reflecting uranium close environment in solid UF_4. As a result uranium electronic structure was interpreted quantitatively and the U $6p$, $5f$ partial electronic densities in uranium tetrafluoride were evaluated experimentally.

II. EXPERIMENTAL

XPS spectra of the solid UF_4 sample were measured with an electrostatic spectrometer HP 5950A Hewlett-Packard using monochromatized Al $K_{\alpha1,2}$ ($h\nu$=1486.6 eV) radiation in a vacuum of 1.3×10^{-7} Pa at room temperature. The device resolution measured as full width (Γ, eV) on the half-maximum (FWHM) of the Au $4f_{7/2}$ peak on the standard rectangular golden plate was 0.8 eV. The binding energies E_b (eV) were measured relative to the binding energy of the C $1s$ electrons from hydrocarbons absorbed on the sample surface accepted to be equal to 285.0 eV. On the gold plate E_b(C $1s$)=284.7 eV at E_b(Au $4f_{7/2}$)=83.8 eV. The FWHM were measured relative to the width of the C $1s$ line of hydrocarbons accepted to be equal to Γ(C $1s$)=1.3 eV. The errors in determination of electron binding energies and the linewidths did not exceed 0.1 eV and that of the relative line intensities was less than 10%.

The UF_4 sample for the XPS studies was prepared from the fine powder ground in the agate mortar as a thick dense flat layer pressed into In on a Ti substrate. The U $4f_{7/2}$ binding energy was measured to be 482.7 eV. Oxygen concentration determined on the basis of O $1s$ XPS peak was found to be less than 4 at. %, which testifies to the low surface oxidation. The CES spectrum was measured with the same spectrometer using an additional accelerating electronic system. A metallic copper substrate with evaporated UF_4 layer for uranium implantation by the electrostatic collection of ^{235m}U recoil atoms resulting from ^{239}Pu decay in the inert atmosphere was used.[12] Peak identification and calibration of the CES was done using the XPS data for UF_4. Elastic scattering related background in the XPS was subtracted by Shirley.[18] For the CES the background was subtracted by Shirley and by exponent. The maximal difference in the relative intensities did not exceed 10%. This work gives the CES spectrum with the background subtracted by exponent (Fig. 1).

The UF_8^{4-} cluster of symmetry group C_{4v} reflecting uranium close environment in solid UF_4 can be constructed if to rotate by 45° an upper cube face with the edge equal to 2.64 Å. Uranium ion located in the center of this cube is surrounded by fluorines located in the cube corners at R_{U-F}=2.29 Å from uranium.[19] The calculation for this cluster was done in the X_α DVM approximation[20,21] based on the Dirac-Slater equation for the four component spinors with
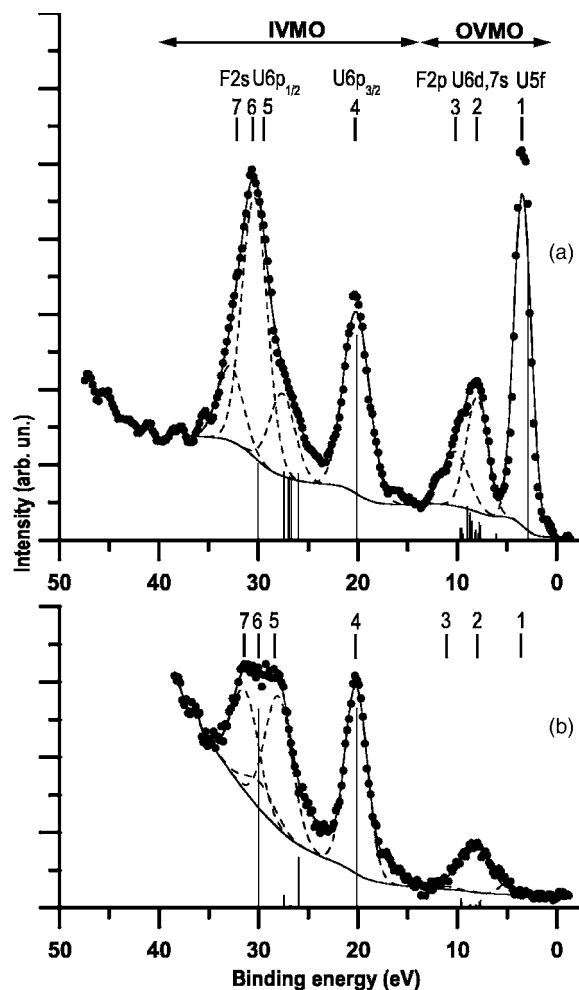

FIG. 1. XPS (a) and CES (b) from solid UF_4. The corresponding theoretical spectra are given under the experimental spectra as vertical bars. The shape of subtracted background and spectra decomposition are shown. The experimental spectral intensities are given in arbitrary units; the theoretical intensities are normalized in %.

exchange-correlation potential.[22] The extended basis of the numerical atomic orbitals (AO) from the solution of Dirac-Slater equation for the isolated atoms beside the filled included the vacant U $7p_{1/2}$, $7p_{3/2}$ states. The basis also took into account the cluster symmetry, i.e., by the technique of projecting operators[20] the regular AOs were reconstructed in the linear combinations converting by the irreducible representations of the binary group C_{4v}. For the relativistic basis calculations an original program of symmetrization was utilized. This program used the matrices of irreducible representations for the most part of binary groups obtained in Ref. 22 and transformation matrices given in Refs. 23 and 24. The numerical diophantine integration during the calculation of the secular equation matrix elements was done by the number of 22 000 points spread in the cluster space. It provided the convergence of MO energies of not worse than 0.1 eV. The local exchange-correlation potential was taken as X_α with α equal to the mean atomic value. Since the clusters were the fragments of the crystal, the ligand AO population renormalization during the self-consisting was done. It allowed an effective account of the stoichiometry and charge

redistribution between the ligands and surrounding crystal.

III. RESULTS AND DISCUSSION

The low binding energy (0–40 eV) XPS from UF_4 can be conditionally subdivided into the two ranges (Fig. 1). The first one 0–15 eV exhibits the structure attributed to the OVMO built mostly from the incompletely filled outer U $5f$, $6d$, $7s$ and F $2p$ AOs (Table I). The second one 15–40 eV shows the IVMO related fine structure. These IVMOs are built mostly from the completely filled inner valence U $2p$ and F $2s$ AOs. The fact that the IVMO XPS parameters correlate with uranium close environment structure in compounds encouraged this subdivision.[8,9,11] The OVMO XPS structure has typical features and can be subdivided into the three components. The IVMO spectral range exhibits pronounced peaks and can be subdivided into the four components (Fig. 1). The low intense shoulders on the lower binding energy side can be attributed to uranium oxide on the sample surface, as well as to the background subtraction imperfection. The areas under these peaks were taken into account. This subdivision allows the qualitative and quantitative comparisons between the XPS, CES and relativistic calculation results for the UF_8^{4-} (C_{4v}) cluster.

Relativistic calculation results are given in Table I. Since the XPS reflect both ground and excited states of ions, the calculated binding energies for the transition (not ground) states must be used[25] for comparison between the theoretical and experimental data. However, it is known[8,11] that in a rough approximation one can suggest that for the valence region the binding energies for the transition state differ from those for the ground state by a constant shift toward the higher absolute energy. Therefore, the present work used the theoretical binding energies increased by 2.87 eV for comparison with the corresponding experimental values (Table II). Taking into account the MO compositions (Table I) and photoionization cross sections σ_i (Ref. 26) (σ_i for the U $7p$ were calculated by Yarjemsky), the theoretical spectral intensities for the considered energy ranges were determined (Table II, Fig. 1). Experimental XPS intensities are given for comparison. A good qualitative agreement between the theoretical and experimental data was obtained (Table II). The worst agreement was reached for the middle ($6\gamma_6-3\gamma_6$) IVMO region.

Earlier[8,9] the IVMO XPS structure of UF_4 was interpreted on the basis of the binding energy differences between the core and valence electronic levels. It enabled us to identify qualitatively the fine spectral structure of UF_4 in the binding energy range 15–40 eV and to attribute it to the IVMO electrons. The relativistic calculation results enabled us to interpret quantitatively the XPS fine structure in the whole range 0–40 eV.

Thus, the sharp peak at 3.8 eV is attributed to the U $5f$ electrons weakly participating in the chemical bond, and the outer valence band—to the outer valence U $5f$, $6d, 7s, 7p$ and F $2p$ AOs and to a lesser degree—to the U $6p$ AO. Earlier[16] experimental evidence for the fact that the $5f$ electrons can participate in the chemical bond in γ-UO_3 without losing their f nature was established. However, for UF_4 such

a strict conclusion could not be made. Thus, the experimental intensity ratios OVMO/IVMO with (and without) taking into account the U $5f$ intensity at 3.8 eV are 0.60 (0.24). It differs slightly from the corresponding theoretical values 0.76 (0.42) (Table II). The theoretical value 0.42 is about twice higher than the corresponding experimental one 0.24 due to the contribution of the U $5f$ electrons. Having attributed, for example, the intensity of the OVMO band only to the U $6d^17s^25f^3$ and 4F $2p^5$ electrons, and the IVMO band—to the U $6p^6$ and 4F $2s^2$ electrons in UF_4, the corresponding theoretical values are 0.78 (0.38). It agrees with the theoretical values 0.76 (0.42), but more than the corresponding experimental values 0.60 (0.24). However, if to attribute the OVMO band to the U $6d^27s^25f^2$ and 4F $2p^5$ electrons, and the IVMO band—to the U $6p^6$ and 4F $2s^2$ electrons, the corresponding theoretical values are 0.62 (0.22). It is in a good agreement with the experimental data. It indicates that the U $5f$ electron involved in the chemical bond is either strongly delocalized or loses its f nature. To the greatest degree, the direct participation of the U $5f$ electrons in the chemical bond was observed in γ-UO_3,[16] and to a lesser degree—in UO_2.[15] Unlike γ-UO_3 and UO_2, in the case of UF_4 this participation can be much lower because of the higher fluorine electronegativity and higher uranium—fluorine interatomic distance. It can result in the delocalization of the U $5f$ electrons and decrease of the U $5f$ photoionization cross section.

In the IVMO XPS range the best agreement in the binding energy was reached only for the $5\gamma_7$, $7\gamma_6(4)$, and $2\gamma_6(7)$ orbitals determining the spectral width. The experimental intensities of peaks and the IVMO group $6\gamma_6-3\gamma_6(6)$ in some cases are much higher than the theoretical values (Table II). Thus, the $6\gamma_6(5)$ and $2\gamma_6(7)$ experimental IVMO intensities are 2.1 and 1.5, respectively. These data do not allow a correct experimental evaluation of the participation degree of these electronic shells in the IVMO formation, since the U $6p_{1/2}$ and F $2s$ photoionization cross section are comparable (Table I).

Taking into account the calculations and experimental core–valence levels binding energy differences for metallic uranium[8] and UF_4, a MO schematic diagram can be built (Fig. 2). This diagram was built in the MO LCAO (molecular orbitals as linear combinations of atomic orbitals) approximation. It enables us to understand the real XPS structure of UF_4. In this approximation one can separate formally the antibonding $5\gamma_7$, $7\gamma_6(4)$, and $6\gamma_6(5)$ and bonding $1\gamma_7$, $3\gamma_6(6)$, and $2\gamma_6(7)$ IVMOs, as well as the quasiatomic (in a certain approximation) $4\gamma_7$, $3\gamma_7$, $2\gamma_7$, $5\gamma_6$, and $4\gamma_6(6)$ IVMOs attributed to the F $2s$ electrons (Fig. 2, Tables I and II). The XPS data show that the binding energies of quasiatomic IVMOs must be close to the magnitude. Indeed, the F $1s$ peak is symmetric, and its FWHM is $\Gamma=1.3$ eV. The F $2s$ binding energy must be about 29.9 eV (Fig. 2). This value is the difference between $E_b=685.3$ eV and $\Delta E_F=655.4$ eV, where E_b is the F $1s$ binding energy in UF_4, and ΔE_F is the difference between the F $1s$ and F $2s$ binding energies for MnF_2 (Ref. 11) (Fig. 2). Theoretical results agree qualitatively with these data (Table II). Since $\Delta E_U=360.6$ eV, $\Delta E_1=362.6$ eV, one can find $\Delta_1=2.0$ eV (Fig. 2). Since the

TABLE I. MO composition and energies E_0[a] (eV) for the UF_8^{4-} (C_{4v}) at $R_{U-F}=2.29$ Å (RX_α DVM), photoionization cross sections σ_i[b] and conversion one-electron partial probabilities α_i[c].

				MO composition												
				U										F		
	MO[d]	Q	$-E_0$, eV	$6s$	$6p_{1/2}$	$6p_{3/2}$	$6d_{3/2}$	$6d_{5/2}$	$7s$	$5f_{5/2}$	$5f_{7/2}$	$7p_{1/2}$	$7p_{3/2}$	$2s$	$2p_{1/2}$	$2p_{3/2}$
			σ_i	1.14	0.89	1.29	0.61	0.55	0.12	3.67	3.48	0.07	0.10	1.44	0.13	0.13
			α_i	0.07	43.38	23.55	6.55	7.71	0.01	0.07	0.04	8.23	4.39			
	$25\gamma_7$	0	−7.18				0.10	0.75		0.01				0.03	0.07	0.04
	$27\gamma_6$	0	−6.93				0.43	0.41			0.01			0.03	0.02	0.10
	$24\gamma_7$	0	−5.46					0.83	0.01	0.01				0.02	0.06	0.07
	$26\gamma_6$	0	−5.21						0.03		0.01	0.91		0.02	0.01	0.02
	$25\gamma_6$	0	−5.07						0.89			0.03		0.03	0.02	0.03
	$23\gamma_7$	0	−4.99				0.71	0.10			0.04			0.01	0.02	0.12
	$22\gamma_7$	0	−4.21			0.01							0.96	0.01		0.02
	$24\gamma_6$	0	−4.20							0.01			0.96	0.01		0.02
	$23\gamma_6$	0	−3.39				0.41	0.44							0.04	0.11
	$21\gamma_7$	0	−1.12				0.04			0.01	0.86				0.06	0.03
O	$20\gamma_7$	0	−0.89					0.02		0.03	0.87				0.02	0.06
	$22\gamma_6$	0	−0.84								0.93	0.01			0.04	0.02
	$21\gamma_6$	0	−0.79				0.01				0.93				0.02	0.04
V	$19\gamma_7$	0	−0.22					0.01		0.86	0.05				0.01	0.07
	$20\gamma_6$	0	−0.03							0.92					0.01	0.07
M	$18\gamma_7$[e]	2	0.00					0.01		0.91	0.01				0.01	0.06
	$19\gamma_6$	2	3.70												0.30	0.70
	$17\gamma_7$	2	4.80			0.06					0.01				0.21	0.72
O	$18\gamma_6$	2	4.85												0.24	0.76
	$17\gamma_6$	2	4.95			0.05				0.02					0.35	0.58
	$16\gamma_7$	2	4.95												0.11	0.89
	$16\gamma_6$	2	4.98												0.54	0.46
	$15\gamma_7$	2	5.03												0.23	0.77
	$14\gamma_7$	2	5.05												0.44	0.56
	$15\gamma_6$	2	5.27			0.01					0.01	0.01	0.01		0.58	0.38
	$13\gamma_7$	2	5.32			0.01							0.03		0.25	0.71
	$14\gamma_6$	2	5.66							0.02	0.02		0.02		0.27	0.67
	$13\gamma_6$	2	5.80		0.01					0.01	0.01	0.02			0.38	0.57
	$12\gamma_6$	2	5.84								0.06				0.36	0.58
	$12\gamma_7$	2	5.85							0.06	0.01				0.24	0.69
	$11\gamma_7$	2	5.88							0.02	0.04				0.45	0.49
	$11\gamma_6$	2	5.91		0.01					0.03	0.02				0.11	0.83
	$10\gamma_7$	2	6.11							0.07	0.02			0.01	0.10	0.80
	$9\gamma_7$	2	6.13							0.01	0.07				0.55	0.37
	$10\gamma_6$	2	6.56	0.01					0.04					0.01	0.33	0.61
	$9\gamma_6$	2	6.70				0.02	0.12						0.01	0.32	0.53
	$8\gamma_7$	2	6.76					0.11						0.01	0.52	0.36
	$7\gamma_7$	2	6.76					0.12						0.01	0.46	0.41
	$8\gamma_6$	2	6.80				0.11	0.01						0.01	0.05	0.82
	$6\gamma_7$	2	2.82				0.13								0.15	0.72
	$5\gamma_7$	2	17.23			0.83							0.01	0.11	0.02	0.03

TABLE I.　(*Continued.*)

				MO composition												
				U										F		
MO^d	Q	$-E_0$, eV σ_i α_i	6s 1.14 0.07	$6p_{1/2}$ 0.89 43.38	$6p_{3/2}$ 1.29 23.55	$6d_{3/2}$ 0.61 6.55	$6d_{5/2}$ 0.55 7.71	7s 0.12 0.01	$5f_{5/2}$ 3.67 0.07	$5f_{7/2}$ 3.48 0.04	$7p_{1/2}$ 0.07 8.23	$7p_{3/2}$ 0.10 4.39	2s 1.44	$2p_{1/2}$ 0.13	$2p_{3/2}$ 0.13
$7\gamma_6$	2	17.23			0.83							0.01	0.11	0.01	0.04
$6\gamma_6$	2	23.09		0.20							0.02		0.78		
I $\quad4\gamma_7$	2	23.81					0.02		0.01				0.97		
$3\gamma_7$	2	23.81				0.01	0.01			0.01			0.97		
V $\quad2\gamma_7$	2	24.00				0.01	0.03						0.96		
$5\gamma_6$	2	24.01				0.02	0.02						0.96		
M $\quad4\gamma_6$	2	24.14	0.01					0.04					0.95		
$1\gamma_7$	2	24.53			0.10							0.01	0.88	0.01	
O $\quad3\gamma_6$	2	24.58			0.10							0.01	0.88		0.01
$2\gamma_6$	2	27.14		0.79									0.19	0.01	0.01
$1\gamma_6$	2	43.29	0.98										0.02		

aCalculated energies are shifted down toward the negative values (down) by 1.8 eV of absolute scale.

bPhotoionization cross section σ_i (Barn per electron) from Ref. 26.

cα_i, relative partial conversion probability per one electron (%) of $E3$ multipole of ^{235}U nucleus with participation of electrons from the nlj shells, determined on the basis of the data from Ref. 27.

dTo simplify the data, all the sequence numbers are shifted like $27\gamma_6 \rightarrow 1\gamma_6$ and $22\gamma_7 \rightarrow 1\gamma_7$, respectively.

eUpper filled orbital $18\gamma_7^-$ (two electrons), filling number for $n\gamma_6^\pm$ and $n\gamma_7^\pm$ MO is 2.

U $6p$ atomic spin-orbit splitting according to the calculation[28] and experimental[29] data is ΔE_{sl}(U $6p$) $=10.0$ eV, the U $6p_{3/2}$ and F $2s$ binding energies are comparable by the magnitude. The $6\gamma_6(5)$ and $2\gamma_6(7)$ IVMO binding energy difference is 4.2 eV. In this case the values characterizing the antibonding Δ_2 and bonding Δ_3 are approximately equal and they are ≈ 2.1 eV (Fig. 2). It agrees with the data on the FWHMs and intensities. Indeed, the intensities of these lines are comparable and FWHM of the antibonding $6\gamma_6(5)$ IVMO is equal to that of the bonding $2\gamma_6(7)$ IVMO. It indicates the compensation of the antibonding (Fig. 2, Table II). Since in the U $6p_{1/2}$–F $2s$ binding energy range the structure is complicated due to the IVMO overlapping, it is very difficult to identify correctly all the IVMOs and to make a conclusion about the contributions of the IVMO electrons to the covalent component of the chemical bond in UF_4.

The conversion transition of the $E3$ multipole for the ^{235m}U nucleus ($T_{1/2} \approx 26$ min) from the first excited state (spin $I_1 = 1/2^+$, $E_1 = 76.5 \mp 0.4$ eV) to the ground nucleus state (spin $I_0 = 7/2^-$, $E_0 = 0$ eV) is accompanied by the low energy electron photoemission. The conversion process is energetically permitted for the U $6s^2 6p^6 5f^3 6d^1 7s^2 7p^0$ electrons. These shells can participate effectively in the OVMO and IVMO formation in uranium compounds. In this case the partial conversion probability per one electron $\alpha_i(EL, I_1 \rightarrow I_0, n_i l_i j_i \rightarrow \varepsilon_i)$ of ejection of $(n_i l_i j_i)$ electron is proportional to the electronic factor $w_e(E3, n_i l_i j_i, h\omega)$, where ε_i, electron kinetic energy; n_i, principal quantum number; l_i and j_i, orbital and total angular moments; and $h\omega$, nucleus excitation energy.[27]

The present work built the theoretical CES spectrum on the basis of the relativistic calculations and relative one-electron partial conversion probabilities[27] [Tables I and II, Fig. 1(b)]. Since the U $6p$ conversion cross section is much higher than that for the other electronic shells (Table I), the CES spectrum from UF_4 reflects rather the U $6p$ partial electronic density. One can see a qualitative agreement between experimental XPS and CES. Also a good agreement between the theoretical and experimental CES spectra was found. Comparison of the XPS and CES data gives three important conclusions. First, the U $6p$ shell participates effectively in the IVMO formation. Second, the U $6p$ shell participates significantly in the OVMO formation. Third, the U $5f$ electrons from the $18\gamma_7^-(1)$ OVMO and electrons from the quasiatomic $4\gamma_7$, $3\gamma_7$, $2\gamma_7$, $5\gamma_6$, and $4\gamma_6(6)$ IVMOs, as expected, practically are not observed at 3.8 and 29.9 eV. The $6\gamma_6(5)$, $1\gamma_7$, $3\gamma_6(6)$, and $2\gamma_6(7)$ IVMO energies differ slightly from the corresponding theoretical values and agree with the experimental XPS parameters (Figs. 1 and 2, Table II).

For comparative quantitative analysis of the experimental and theoretical intensities the considered spectra were decomposed with the data of Fig. 2 in mind. The diagram of Fig. 2 was built on the basis of the experimental binding energy differences and theoretical intensities. The identification of the XPS and CES structures is reflected in Table II and Fig. 3. These data show that the experimental XPS and CES binding energies practically coincide to within the measurement errors. However, the experimental IVMO intensities often differ from the corresponding theoretical ones. The best agreement was reached for the $5\gamma_7$, $7\gamma_6(4)$ IVMOs. Taking into account conversion cross sections and experimental

TABLE II. XPS and CES parameters for the UF_8^{4-} (C_{4v}) cluster at R_{U-F}=2.29 Å (RX_{α} DVM), and the experimental density $\rho_i(e^-)$ of U $6p$ electronic states in UF_4.

	MO	$-E^a$, eV	XPS Energy[b], eV Experiment	XPS Intensity, % Theory	XPS Intensity, % Experiment	CES Energy[b], eV Experiment	CES Intensity, % Theory	CES Intensity, % Experiment	ρ_i, e^- units U $6p_{3/2}$	U $6p_{1/2}$
	$18\gamma_7$[c]	2.87	3.8(1.5)[d]	20.9	22.4		0.1			
	$19\gamma_6$	6.07		0.4		5.3(1.4)		0.8		
	$17\gamma_7$	7.67		1.0			1.4			
	$18\gamma_6$	7.72		0.4						
	$17\gamma_6$	7.82		1.2			1.1			
	$16\gamma_7$	7.82		0.4						
	$16\gamma_6$	7.85		0.4						
	$15\gamma_7$	7.90		0.4						
	$14\gamma_7$	7.92		0.4						
O	$15\gamma_6$	8.14	8.0(2.5)	0.7	9.3		0.4			
	$13\gamma_7$	8.19		0.5		8.2(3.7)	0.4	10.1		
V	$14\gamma_6$	8.53		1.3			0.1			
	$13\gamma_6$	8.67		0.9			0.6			
M	$12\gamma_6$	8.71		1.6						
	$12\gamma_7$	8.72		1.9						
O	$11\gamma_7$	8.75		1.7						
	$11\gamma_6$	8.78		1.5			0.5			
	$10\gamma_7$	8.98		2.3						
	$9\gamma_7$	9.00		2.0						
	$10\gamma_6$	9.43		0.4						
	$9\gamma_6$[c]	9.57		0.8			1.0			
	$8\gamma_7$	9.63		0.7			0.8			
	$7\gamma_7$	9.63		0.8			0.9			
	$8\gamma_6$	9.67		0.8			0.8			
	$6\gamma_7$	9.69	10.2(3.2)	0.8	5.6	11.1(2.4)	0.9	0.4		
	ΣI_i^e			44.2	37.3		9.0	11.3	0.5	0.1
	$5\gamma_7$	20.10	20.1(2.5)	7.1	9.8	20.2(2.7)	19.0	16.9		
	$7\gamma_6$	20.10	20.1(2.5)	7.1	9.9	20.2(2.7)	19.0	16.9	2.9	
I	$6\gamma_6$	25.96	27.6(3.0)	4.6	9.5	28.0(3.2)	9.6	25.7		1.0
	$4\gamma_7$	26.68		4.6			0.2			
V	$3\gamma_7$	26.68		4.6			0.1			
	$2\gamma_7$	26.87		4.4			0.3			
M	$5\gamma_6$	26.88	30.4(3.0)	4.4	25.4		0.3			
	$4\gamma_6$	27.01		4.3						
O	$1\gamma_7$	27.40		4.7		29.8(3.5)	2.3	3.3		
	$3\gamma_6$	27.45		4.7		29.8(3.5)	2.3	3.3	0.6	
	$2\gamma_6$	30.01	31.8(3.0)	5.3	8.1	31.4(3.2)	37.9	23.2		0.9
	ΣI_i^e			55.8	62.7		91.0	88.7	3.5	1.9
	$1\gamma_6$	46.16	48.3(6.0)	≈7.1			≈0.1			

[a]Calculated energies are shifted down toward the negative energies by 2.87 eV so that the calculated energy of the $5\gamma_7$ IVMO would be 20.1 eV.

[b]FWHMs in eV are given in the parentheses.

[c]Upper filled MO $18\gamma_7$ (two electrons), filling number for the $n\gamma_6$ and $n\gamma_7$ MOs is 2.

[d]FWHM is given relative to the Γ(C $1s$)=1.3 eV.

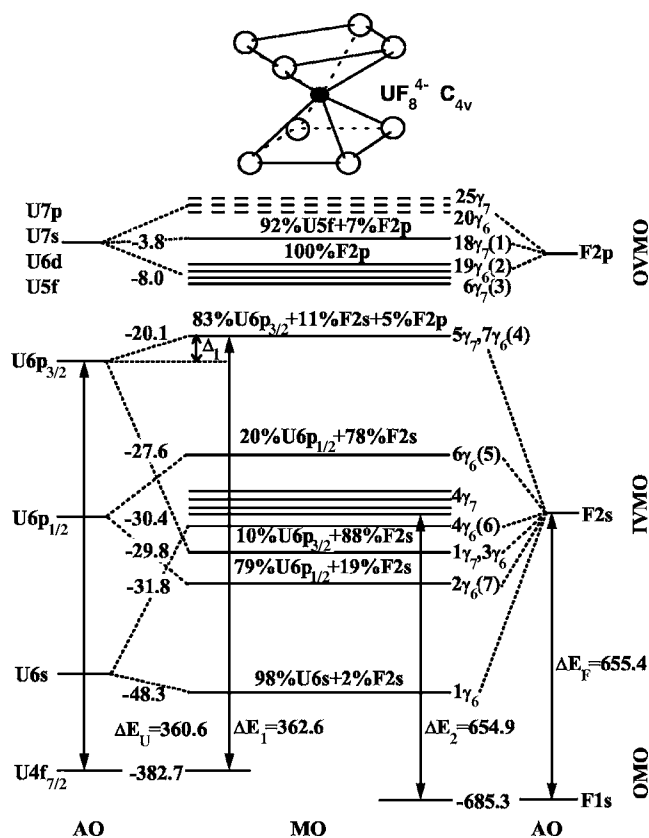[e]Total intensities and the U $6p$ electronic state densities.

FIG. 2. MO schematic diagram for the UF_8^{4-} (C_{4v}) cluster built taking into account the theoretical and experimental data. The chemical shift during the cluster formation is not shown. The arrows indicate some experimentally measurable binding energy differences. The experimental binding energies (eV) are given to the left side. Energetic scale is not kept.
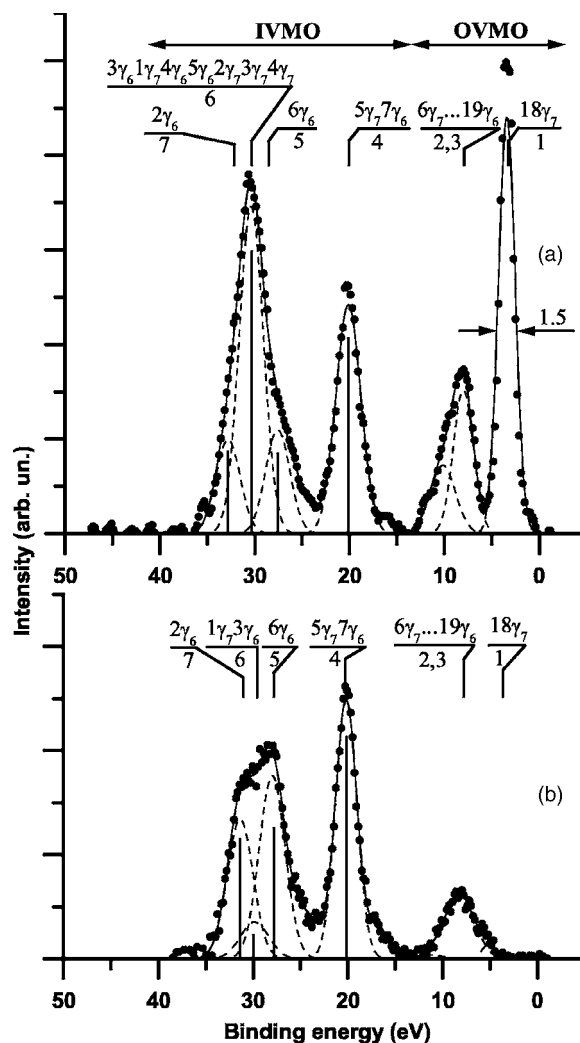

FIG. 3. XPS (a) and CES (b) from UF_4 with subtracted background. The corresponding expected spectra obtained on the basis of the theoretical and experimental data are given under the experimental spectra as vertical bars. The spectral intensities are given in arbitrary units; the theoretical intensities are normalized in %.

intensities, the partial U $6p_{3/2,1/2}$ electronic density in solid UF_4 was evaluated (Table II).

Evaluation of the number of the U $6p_{3/2,1/2}$ electrons participating in the chemical bond in UF_4 was done in the following approximation. The $5\gamma_7$, $7\gamma_6(4)$ and $1\gamma_7$, $3\gamma_6(6)$ IVMO CES intensity was suggested to be formed only by the U $6p_{3/2}$ electrons, while the $6\gamma_6(5)$ and $2\gamma_6(7)$ one—only by the U $6p_{1/2}$ electrons. This suggestion is well grounded (see Table I). While considering the theoretical intensities ratio first it was suggested that the $5\gamma_7$, $7\gamma_6(4)$ IVMOs are populated by the 3.32 U $6p_{3/2}$ electrons and the $6\gamma_6(5)$ and $2\gamma_6(7)$ IVMOs—by the 2.0 U $6p_{1/2}$ electrons (Table I). After that, the changes in the intensities were renormalized taking into account the experimental data. Also, on the basis of the analysis of the experimental and theoretical data it was suggested that the relative CES intensity at 8.2 eV, being 11.3 (Table II) had a 6.35 contribution from the U $6p$ electrons [see Tables I and II, Fig. 1(b)]. As a result it was found that the OVMOs include 0.6 U $6p$ electrons (Table II). It is more than the corresponding theoretical value 0.3 electrons (Table I). In the beginning it was also suggested that mainly the U $6p_{3/2}$ electrons participate in the OVMO formation. Table I shows that the $6p_{1/2}$ contribution to the OVMO is about 6 times lower. Therefore, 0.1 U $6p_{1/2}$ electrons were suggested to be spread around among the OVMOs. The remaining

1.9 U $6p_{1/2}$ electrons were suggested to be spread among the $6\gamma_6(5)$ and $2\gamma_6(7)$ taking into account their intensities.

In the IVMO energy range a significant difference between the theoretical and experimental data was observed. For example, the antibonding $5\gamma_7$, $7\gamma_6(4)$ IVMO contains 2.9 U $6p_{3/2}$ electrons, which is less than the corresponding calculated value 3.32 (Table I). The difference was also observed for the bonding $1\gamma_7$, $3\gamma_6(6)$ IVMO: 0.6 electrons, experiment (Table II); and 0.4, theory (Table I). For the antibonding $6\gamma_6(5)$ and bonding $2\gamma_6(7)$ the corresponding experimental and theoretical values are 1.0 and 0.4 electrons for the $6\gamma_6(5)$; 0.9 and 1.58 for the $2\gamma_6(7)$. These data show that the IVMO formation (AO mixing) in reality takes place in a much higher scale (13%–60%) than it was predicted by the theory.

The quantum mechanics can predict qualitatively the alterations of the considered spectral intensities depending on the binding energy. Therefore, one can vary the initial data for the initial clusters for the better agreement between the

theoretical and experimental data. As it was shown in Ref. 9, the wider a MO peak is, the more its electrons participate (bonding, antibonding) in the chemical bond. The lines $5\gamma_7$, $7\gamma_6(4)$ corresponding to the antibonding IVMOs in the CES are observed narrower than the corresponding bonding $1\gamma_6$, $3\gamma_6(6)$ IVMO (Table II). It must be noted that the $5\gamma_7$, $7\gamma_6(4)$ XPS peak was calibrated, which cannot be done for the CES peak. The observed relative decrease of the $5\gamma_7$, $7\gamma_6(4)$ IVMO FWHM comparing to the corresponding bonding $1\gamma_7$, $3\gamma_6$ IVMO FWHM can be explained by the contribution from, for example, the F $2p$ and U $7p$ AOs in the $5\gamma_7$, $7\gamma_6(4)$ IVMO. As it was shown earlier for the XPS analysis, it leads to the loss of the antibonding nature of this IVMO. Comparison of the experimental (16.9%) and theoretical (19.0%) $5\gamma_7$, $7\gamma_6(4)$ IVMO intensity shows that the contribution from the U $6p_{3/2}$ AO to this IVMO was theoretically overestimated. The experimental (25.7%) contribution from the U $6p_{1/2}$ AO to the $6\gamma_6(5)$ IVMO is significantly higher than the theoretical one (9.6%), and the contribution (23.2%) of this AO to the $2\gamma_6(7)$ IVMO is significantly lower than the theoretical one (37.9%). It indicates that in reality the degree of participation of the U $6p_{1/2}$ AO in the IVMO formation is about 2 times higher as it follows from the theoretical results. As it follows from the XPS and CES data, $6\gamma_6(5)$ and $2\gamma_6(7)$ IVMO peaks are about equal by the intensity. It indicates about equal contribution from the $6p_{1/2}$ and O $2s$ AOs to this IVMO.

The obtained data for the first time allowed an experimental determination of the IVMO composition in UF_4. Thus, the bonding $2\gamma_6(7)$ and the corresponding antibonding $6\gamma_6(5)$ IVMOs were found to form mostly from the U $6p_{1/2}$ and F $2s$ AOs. The calculated compositions of these shells (79% of the U $6p_{1/2}$ and 19% of the F $2s$ AOs and 20% of the U $6p_{1/2}$ and 78% of the F $2s$ AOs) differ significantly from the experimental compositions (45% of the U $6p_{1/2}$ and 55% of the F $2s$ AOs and 50% of the U $6p_{1/2}$ and 50% of the F $2s$ AOs). The bonding $1\gamma_7$, $3\gamma_6(6)$ and the corresponding antibonding $5\gamma_7$, $7\gamma_6(4)$ IVMOs were found to form mostly from the U $6p_{3/2}$ and F $2s$ AOs, and their calculated compositions (10% of the U $6p_{3/2}$ and 88% of the F $2s$ AOs and 83% of the U $6p_{3/2}$ and 11% of the F $2s$ AOs) differ less from the experimental compositions (15% of the U $6p_{3/2}$ and 85% of the F $2s$ AOs and 73% of the U $6p_{3/2}$ and 27% of the F $2s$ AOs) (Tables I and II).

The most ambiguous for interpretation is the $4\gamma_7-3\gamma_6(6)$ IVMO XPS region. Comparison of the XPS and CES data shows that the structure in this range in general is formed from the F $2s$ electrons. It agrees with the calculation results. However, the U $6p$-F $2s$ AO overlap during formation of $5\gamma_7$, $7\gamma_6(4)$ and $1\gamma_7$, $3\gamma_6(6)$ IVMOs was underestimated, but the IVMO sequence order was determined correctly. The knowledge on the correct IVMO sequence order is critical for understanding of the IVMO contributions to the covalent component of the chemical bond in UF_4.

In conclusion we would like to note that despite the approximation imperfections, the calculation results for the UF_8^{4-} (C_{4v}) cluster reflecting uranium close environment in solid UF_4 are in a satisfactory agreement with the experimental data. It allowed for a reliable identification of the peaks of the U $5f$ electrons weakly participating in the chemical bond, as well as the IVMO electrons. These results can be also used for the interpretation of other x-ray spectra (Auger, emission, absorption, etc.[8]) of uranium compounds.

IV. CONCLUSIONS

Low binding energy (0–40 eV) x-ray photoelectron and conversion electron spectra of UF_4 were measured and interpreted in the relativistic X_α discrete variation approximation for the UF_8^{4-} (C_{4v}) cluster reflecting uranium close environment in solid UF_4. It yielded a satisfactory qualitative and in some cases quantitative agreement between the theoretical and experimental data.

It is theoretically shown that in $UF_4 \approx 1$ U $5f$ electron can directly participate in formation of chemical bond. The experimental evaluation, however, has shown that the U $5f$ electron in UF_4 is more delocalized in the OVMO binding energy range from -5 to -11 eV and less maintains the f nature than in γ-UO_3 and UO_2. About 2 U $5f$ electrons weakly participating in the chemical bond are localized at -3.8 eV, and the vacant U $5f$ electronic states are generally delocalized in the low positive energy range (0–7 eV).

The U $6p$ electrons (0.6 U $6p$ electrons) were experimentally shown to participate significantly in the OVMO formation beside the IVMO formation. It agrees with the theoretical data.

The peaks in the binding energy range 0–40 eV in the studied spectra were identified, the IVMO sequence order and quantitative experimental compositions were determined. The bonding $2\gamma_6(7)$ and corresponding antibonding $6\gamma_6(5)$ IVMO were determined to form mostly from the U $6p_{1/2}$ and F $2s$ atomic shells, and their calculated compositions (79% of the U $6p_{1/2}$ and 19% of the F $2s$ AOs and 20% of the U $6p_{1/2}$ and 78% of the F $2s$ AOs) were found to differ significantly from the experimental compositions (45% of the U $6p_{1/2}$ and 55% of the F $2s$ AOs and 50% of the U $6p_{1/2}$ and 50% of the F $2s$ AOs). The bonding $1\gamma_7$, $3\gamma_6(6)$ and the corresponding antibonding $5\gamma_7$, $7\gamma_6(4)$ IVMOs were found to form mostly from the U $6p_{3/2}$ and F $2s$ AOs, and their calculated compositions (10% of the U $6p_{3/2}$ and 88% of the F $2s$ AOs and 83% of the U $6p_{3/2}$ and 11% of the F $2s$ AOs) differ less from the experimental compositions (15% of the $6p_{3/2}$ and 85% of the F $2s$ AOs and 73% of the U $6p_{3/2}$ and 27% of the F $2s$ AOs).

*Electronic address: teterin@ignph.kiae.ru

†Electronic address: ryz@ihim.uran.ru

‡Electronic address: vukac@rc.pmf.cg.ac.yu

[1] B. W. Veal, D. J. Lam, W. T. Carnall, and H. R. Hoekstra, Phys. Rev. B **12**, 5651 (1975).

[2] J. J. Pireaux, N. Martensson, R. Didriksson, and K. Siegbahn, Chem. Phys. Lett. **46**, 215 (1977).

[3] Y. A. Teterin, V. M. Kulakov, A. S. Baev, A. G. Zelenkov, N. B. Nevzorov, I. V. Melnikov, V. A. Streltsov, L. G. Mashirov, and D. N. Suglobov, Sov. Phys. Dokl. **255**, 434 (1980).

[4] J. M. Dyke, G. D. Josland, A. Morris, P. M. Tucker, and J. W. Tyler, J. Chem. Soc., Faraday Trans. 2 **77**, 1273 (1981).

[5] E. Thibaut, J.-P. Boutique, J. J. Verbist, J.-C. Levet, and H. Noel, J. Am. Chem. Soc. **104**, 5266 (1982).

[6] C. P. Opeil, R. K. Schulze, M. E. Manley *et al.*, Phys. Rev. B **73**, 165109 (2006).

[7] Y. A. Teterin, V. A. Terehov, M. V. Ryzhkov, I. O. Utkin, K. E. Ivanov, A. Y. Teterin, and A. S. Nikitin, J. Electron Spectrosc. Relat. Phenom. **114-116**, 915 (2001).

[8] Y. A. Teterin and A. Y. Teterin, Russ. Chem. Rev. **73**, 541 (2004).

[9] Y. A. Teterin and S. G. Gagarin, *Inner Valence Molecular Orbitals and the Influence of Their Electrons on the Chemical Bond Nature in Compounds* (TsNIIatoinform, Moscow, 1985), in Russian.

[10] Y. A. Teterin and S. Gagarin, Russ. Chem. Rev. **65**, 895 (1996).

[11] Y. A. Teterin and A. Y. Teterin, Russ. Chem. Rev. **71**, 347 (2002).

[12] A. D. Panov, V. I. Zhudov, and Y. A. Teterin, J. Struct. Chem. **39**, 1048 (1998).

[13] K. E. Ivanov, D. K. Shuh, Y. A. Teterin, A. Y. Teterin, S. M. Butorin, J.-H. Guo, M. Magnuson, and J. Nordgren, *Book of Abstracts Fifth General Conference of the Balkan Physical Union BPU-5. SO06-014* (Vrnjacka Banja, Serbian Physical Society, Serbia, 2003), p. 100.

[14] T. Mukoyama, H. Nakamatsu, and H. Adachi, J. Electron Spectrosc. Relat. Phenom. **63**, 409 (1993).

[15] Y. A. Teterin and A. Y. Teterin, Nucl. Technol. Radiat. Prot. **19**, 3 (2004).

[16] Y. A. Teterin, M. V. Ryzhkov, A. Y. Teterin, A. D. Panov, A. S. Nikitin, K. E. Ivanov, and I. O. Utkin, Radiochemistry (Moscow, Russ. Fed.) **44**, 224 (2002).

[17] I. O. Utkin, Y. A. Teterin, V. Terekhov, M. V. Ryzhkov, A. Y. Teterin, and L. Vukcevic, Radiochemistry (Moscow, Russ. Fed.) **47**, 334 (2005).

[18] D. A. Shirley, Phys. Rev. B **5**, 4709 (1972).

[19] Y. V. Gagarinsky and L. A. Hripin, *Uranium Tetrafluoride* (Atomizdat, Moscow, 1966).

[20] A. Rosen and D. E. Ellis, J. Chem. Phys. **62**, 3039 (1975).

[21] H. Adachy, Technical Report No. 27(1364–1393), Osaka University, 1977.

[22] O. Gunnarsson and B. I. Lundqvist, Phys. Rev. B **13**, 4274 (1976).

[23] P. Pyykko and H. Toivonen, Acta Acad. Aboensis, Ser. B **43**, 1 (1983).

[24] D. A. Varshalovich, A. N. Moskalev, and V. K. Khersonskii, *Quantum Theory of Angular Momentum* (World Scientific, Singapore, 1988).

[25] J. C. Slater and K. H. Johnson, Phys. Rev. B **5**, 844 (1972).

[26] I. M. Band, Y. I. Kharitonov, and M. B. Trzhaskovskaya, At. Data Nucl. Data Tables **23**, 443 (1979).

[27] D. P. Grechukhin and A. Soldatov, Sov. J. Nucl. Phys. **28**, 622 (1978).

[28] K. N. Huang, M. Aojogi, M. N. Chen, B. Graseman, and H. Mark, At. Data Nucl. Data Tables **18**, 243 (1976).

[29] J. S. Fugle, A. F. Burr, L. M. Watsson, D. Y. Fabian, and W. Laaang, J. Phys. F: Met. Phys. **4**, 335 (1974).